Bioorg. Med. Chem. 78 (2023) 117136

Contents lists available at ScienceDirect

Bioorganic & Medicinal Chemistry

journal homepage: www.elsevier.com/locate/bmc

Improved synthesis of deoxyalpinoid B and quantification of antileishmanial activity of deoxyalpinoid B and sulforaphane

Emma Leary [a], Ethan T. Anderson [a], Jasmine K. Keyes [b], Tristan R. Huskie [b], David J. Blake [a], Kenneth A. Miller [b,*]

[a] Department of Biology, Fort Lewis College, 1000 Rim Drive, Durango, CO 81301, United States
[b] Department of Chemistry and Biochemistry, Fort Lewis College, 1000 Rim Drive, Durango, CO 81301, United States

ARTICLE INFO

Keywords:
Leishmaniasis
Deoxyalpinoid B
Sulforaphane
Meyer-Schuster rearrangement
Leishmania donovani
Leishmania infantatum

ABSTRACT

The total synthesis and antileishmanial activity of deoxyalpinoid B is reported via a cationic gold-catalyzed Meyer-Schuster rearrangement. The activity of deoxyalpinoid B and a known inducer of oxidative stress, sulforaphane, against *Leishmania donovani* and *Leishmania infantatum* are both reported for the first time. Both compounds exhibit potent antileishmanial activity against both species. We hypothesize that the activation of intracellular oxidative stress is a key molecular response for the inhibition of *Leishmania*.

1. Introduction

Leishmaniasis is a vector-borne tropical disease transmitted by sandflies and caused by a protozoan parasite that spans over 20 *Leishmania* species and is contracted by 700,000–1 million people each year, killing >50,000 people annually.[1] According to the World Health Organization, leishmaniasis is one of the seven most important tropical diseases and is the single most neglected in terms of new drug development.[1] Visceral leishmaniasis (VL), the deadliest of three clinical forms of leishmaniasis, causes fever and damage to the spleen and liver. VL is the second largest parasitic killer in the world after malaria, and if left untreated VL infections inevitably result in death.[1] The current first line treatments for VL infections are small molecules such as amphotericin B (AMB),[2] paromomycin, miltefosine, pentamidine or pentavalent antimonials.[3] While these drugs can be effective, they are highly toxic, not well tolerated by patients, must generally be given intravenously, and are increasingly ineffective due to drug resistant strains of the parasite.[2] The grave prognosis of untreated VL infections and lack of safer alternatives are the only reason these drugs remain in use. No vaccines or novel drugs to treat leishmaniasis are currently in the clinic. New small molecule treatments for this disease are urgently needed, but given the patient population, there is little financial incentive for for-profit pharmaceutical companies to devote financial resources to these efforts.

Recent work indicates that plant metabolites that increase reactive oxygen species (ROS) can be quite effective antileishmanials, and several of these compounds pose minimal toxicity to human cells.[4] Alpinoids are compounds derived from the plant *Alpinia officinarum*, a medicinal herb native to East Asia.[5] Interest in the alpinoids has increased of late due to the discovery of the potent anticancer activity displayed by deoxyalpinoid B (DAB), **1**, and *in vitro* cancer cytotoxicity of **1** was attributed to oxidative stress and ROS generation (Fig. 1).[6] Sulforaphane (SFN) is an isothiocyanate agent derived from cruciferous vegetables such as broccoli and potently up-regulates the expression of cytoprotective and antioxidant genes via the NRF2 transcription factor.[7,8] SFN acts intracellularly by generating reactive oxygen species (ROS) that modify at least four cysteine residues of KEAP1, which is the cytosolic inhibitor of NRF2, including Cys151 to form reversible thionoacyl adducts thereby modifying the redox-sensitive sulfhydryl groups on the KEAP1 protein. These modified sulfhydryl groups release NRF2 from KEAP1 and lead to the expression of NRF2-mediated transcriptional activity.[9,10] SFN has been shown to increase the expression of >70 cytoprotective and antioxidant genes in an NRF2-dependent manner[11] and can inhibit *de novo* synthesis of pro-inflammatory cytokines in response to cigarette smoke.[12] We hypothesize that compounds that generate oxidative stress can reduce leishmanial viability and infectivity and given the urgent need for new treatments for leishmaniasis, studies to synthesize and evaluate **1** for antileishmanial activity were

* Corresponding author.
E-mail address: miller_k@fortlewis.edu (K.A. Miller).

https://doi.org/10.1016/j.bmc.2022.117136
Received 25 August 2022; Received in revised form 17 October 2022; Accepted 13 December 2022
Available online 18 December 2022

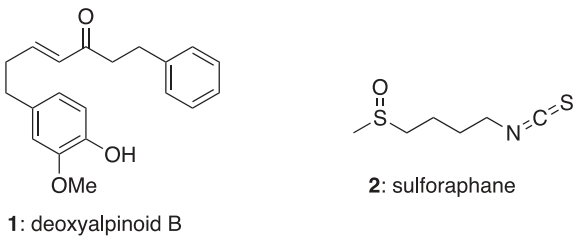

Fig. 1. The structure of deoxyalpinoid B and sulforaphane.

undertaken. Within this context, identical experiments to evaluate the antileishmanial activity of sulforaphane were also undertaken.

Previous syntheses of alpinoids such as **1** and other related diarylheptanoids have focused on two main approaches. Most commonly cross metathesis of a terminal alkene with a terminal α,β-unsaturated ketone[5] or reaction of a stabilized phosphorous ylide with an aldehyde have been employed to create the internal alkene in these natural products.[13] Cross metathesis suffers from the need to use a large excess of one alkene coupling partner, moderate yields, and the need for expensive ruthenium catalysts, and high catalyst loading. To begin to address these drawbacks and in an effort to develop a flexible approach that would enable the rapid synthesis of alpinoid analogs, the gold-catalyzed Meyer-Schuster rearrangement presented several advantages as a method to install the key α,β-unsaturated ketone unit in these compounds.[14,15]

2. Results/discussion

Synthesis of deoxyalpinoid B (DAB) commenced with protection of eugenol as the corresponding silyl ether **4** (Scheme 1). Hydroboration/oxidation led to the primary alcohol **5** followed by PCC oxidation to deliver the known aldehyde **6**.[16] The propargylic alcohol **7** was obtained by addition of the lithium acetylide of 4-phenyl-1-butyne to this aldehyde. Following the procedure of Sheppard and coworkers, propargylic alcohol **7** underwent efficient Meyer-Schuster rearrangement when treated with 1 % of the commercially available gold catalyst PPh_3AuNTf_2 in toluene and one equivalent of MeOH.[17] In the event, the key α,β-unsaturated ketone in **8** was installed in excellent yield and >20:1 E:Z selectivity. Standard deprotection of the TIPS group gave deoxyalpinoid B (**1**) for which NMR spectral data ^1H and ^{13}C NMR) were identical to those previously reported.[18]

Prior to determining the antimicrobial properties of DAB and SFN against different species of *Leishmania*, THP-1 viability was assessed via a dose response curve. THP-1 cells were exposed to 1, 5, 10, 50 and 100 μM SFN or DAB for 48 h, and viability was quantified as described in Methods. At 5 μM, SFN and DAB decreased THP-1 viability to 84 % and 79 % respectively. At 10 μM both compounds decreased viability equally to approximately 76 %. At concentrations of 50 and 100 μM, DAB was significantly more cytotoxic to THP-1 cells than SFN leading to the total loss of viability, whereas SFN at higher concentrations lead to <45 % viability (Fig. 2). Understanding that selective toxicity is important in the development of antileishmanial compounds, 10 μM was selected as an appropriate concentration to assess the intracellular antileishmanial activity of SFN and DAB.

To identify the inhibitory effects of synthesized DAB and natural compounds such as SFN against *Leishmaniasis*, infectious metacyclic promastigotes were incubated with various concentrations of DAB or SFN for 48 h. The parasites were then assessed for metabolic activity as

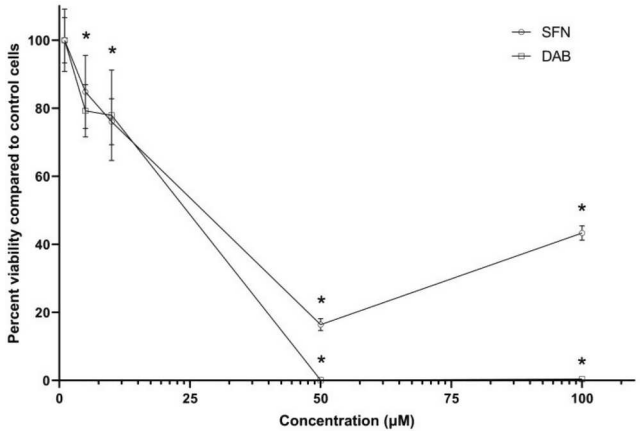

Fig. 2. THP-1 cell viability in the presence of sulforaphane or deoxyalpinoid B. THP-1 cells were incubated with various concentration of SFN or DAB for 48 h and viability was quantified through a modified MTT assay. Data presented are mean percent viability ± SD. Asterisks indicate a significant difference compared to controls cells not exposed to any compound ($P < 0.05$). The experiment was repeated at least four times (≥4 biological replicates).

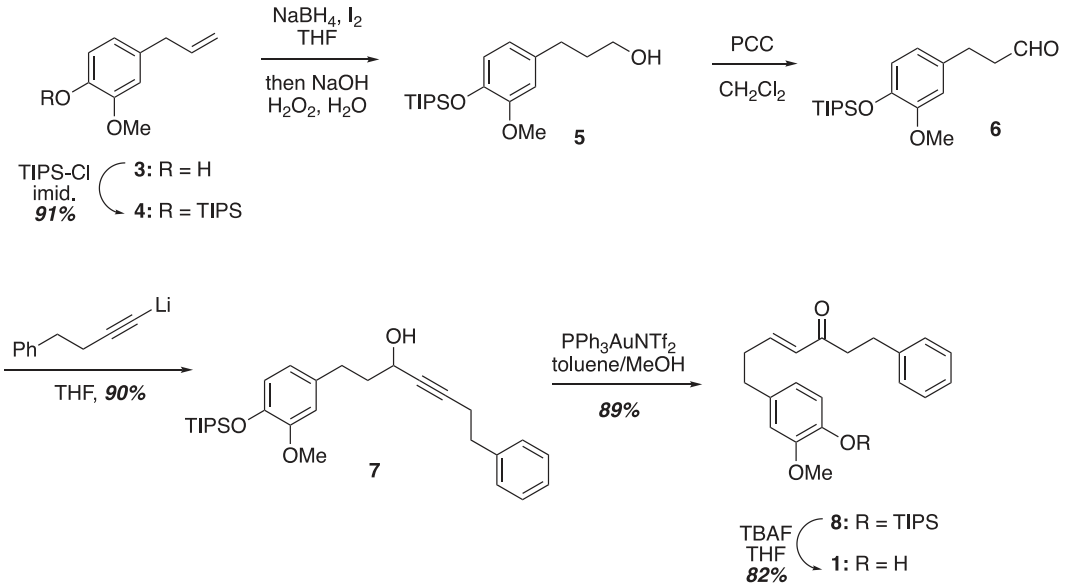

Scheme 1. The synthesis of deoxyaplinoid B.

previously described using a modified MTT assay.[19] Untreated promastigotes, which served as a negative control, were normalized to 100 % viability. AMB treatment was used as a positive control at the IC_{50} concentration of 0.5 μM[20] and led to a significant reduction in viability (Fig. 3). AMB binds preferentially to ergosterol, which is the major sterol of *Leishmaniasis*, and affects membrane integrity to exert its anti-leishmanial action, which is independent of cell-mediated parasiticidal mechanisms.[16,21] The IC_{50} concentration of DAB against LD was quantified as 21.4 μM and the IC_{50} concentration of SFN against LD was 23.3 μM. Promastigote viability was reduced to approximately 50 % at a final concentration of 10 μM of both DAB and SFN (43 % and 57 %, respectively). Promastigote viability was eliminated (<10 % viable) at a final concentration of 50 μM of both DAB and SFN suggesting that these compounds were highly effective against promastigote growth of *Leishmania donovani.* Promastigote viability was also assessed against *Leishmania infantatum,* which is a second species that causes VL, using the same concentrations of DAB, SFN and AMB that lead to equivalent inhibition of promastigote growth after 48 h (Fig. 4). The IC_{50} concentrations against LI were 22.0 μM for DAB and 16.5 μM for SFN. These data support the hypothesis that DAB and SFN can inhibit promastigote viability possibly by altering the levels of oxidative stress in *Leishmania* species.

To provide evidence for the hypothesis that these natural products increase oxidative stress in *Leishmania* parasite, LD promastigotes were loaded with two different compounds, H_2DCFA or Mito Sox, and then were exposed to DAB and SFN (10 and 50 μM) or AMB (0.5 μM) for 24 h (Fig. 5). DAB at both concentrations tested led to a substantial, significant increase in both intercellular ROS as quantified by H_2DCFA fluorescence and mitochondrial superoxide as quantified by Mito Sox fluorescence (Fig. 5). Alternatively, SFN increased intercellular ROS only at 10 μM as quantified by H_2DCFA fluorescence. These results indicate that although both compounds increased ROS within the promastigote, the increase in both cellular ROS and mitochondrial superoxide produced by DAB was significantly higher than ROS produced using SFN indicating a higher level of oxidative stress in DAB-treated promastigotes. Ligand-protein interaction studies have identified that SFN can also interact with the KMP11 protein within the flagellum of *Leishmania donovani* and therefore has been hypothesized to be implicated in the treatment of leishmaniasis in humans.[22] This study is the first to confirm that SFN tested *in vitro* has antileishmanial activity.

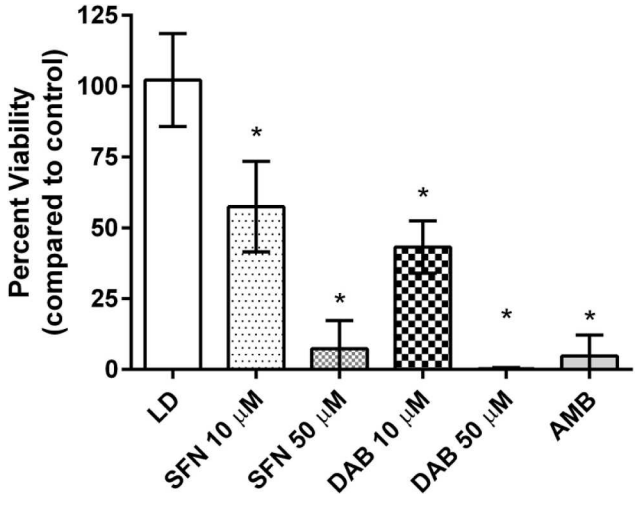

Fig. 3. Promastigote viability of *Leishmania donovani*. Promastigotes were incubated with either SFN, DAB or AMB for 48 h and viability was quantified through a modified MTT assay. Data presented are mean percent viability ± SEM. Asterisks indicate a significant difference compared to controls cells not exposed to any compound ($P < 0.05$). The experiment was repeated at least four times (≥4 biological replicates).

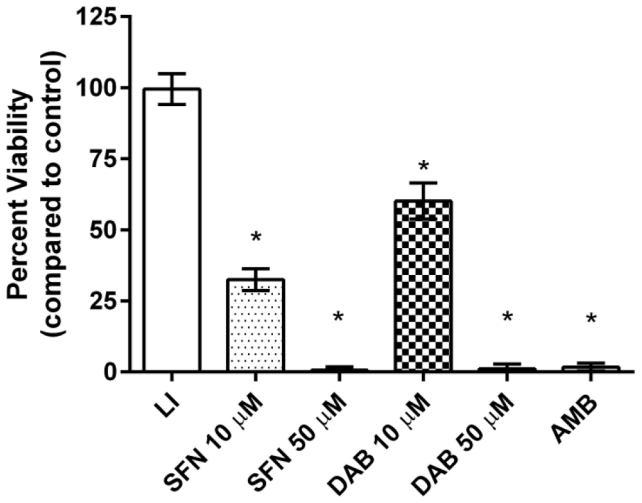

Fig. 4. Promastigote viability of *Leishmania infantatum*. Promastigotes were incubated with either SFN, DAB or AMB for 48 h and viability was quantified through a modified MTT assay. Data presented are mean percent viability ± SEM. Asterisks indicate a significant difference compared to controls cells not exposed to any compound ($P < 0.05$). The experiment was repeated at least four times (≥4 biological replicates).

To identify the cellular expression patterns activated in human macrophages by DAB and SFN as potential anti-parasitic compounds in the presence and absence of *Leishmania donovani*, whole RNA transcriptomic analysis was completed. Differentiated THP-1 cells were infected as described below, then cells were exposed to 10 μM DAB, 10 μM SFN, or 0.5 μM AMB for 18 h. This intermediate time point was chosen to determine what intracellular transcriptional pathways were activated. *Leishmania donovani* infection led to increased expression of metallothionein (MTs) genes in THP-1 cells (FC > 2, $P < 0.005$) specifically MT1G, MT2A, MT1E and MT1F (Table S1) as previously described.[23,24] Overall, the mineral absorption pathway was significantly changed (FC > 10, $P < 0.005$) after infection as confirmed through KEGG analysis. Metallothioneins are small, cysteine-rich and heavy metal-binding proteins, which participate in an array of protective stress responses including oxidative stress.[25] *Leishmania donovani* infection also led to a significant increase in expression of heme oxygenase 1 (OH-1) [$\log_2$FC = 0.839] and ATF3 [$\log_2$FC = 0.209] as previously described.[26] Alternatively, a significant reduction in the expression of NRF2 was observed at the given timepoint [$\log_2$FC = -0.252] possibly indicating a negative feedback mechanism post-infection. SFN is a well-known NRF2 activator and a master regulator of oxidative stress in cells[8] and at micromolar concentrations can lead to antioxidant and anti-inflammatory responses in cells. As expected, SFN treatment increased the expression of numerous NRF2-dependent genes including cytochrome P450 and aldo–keto reductase[27,28] and the pathways in cancer were significantly altered (FC > 10, $P < 0.005$) as previously described (Table S2).[29] DAB treatment increased expression of heat shock protein (HSP) A6 and A7 and the Hes family transcription factor 7 (Table S3), which accounts for ten percent of the genes involved in the PI3K pathway. KEGG analysis also indicated that cytokine-cytokine receptor interactions and neuroactive ligand-receptor interactions were significantly different in human macrophages after both SFN and DAB treatment. The neuroactive ligand-receptor interactions were activated after *Leishmania donovani* infection in both SFN and DAB treatment indicating this pathway may be necessary to inhibit *Leishmania donovani* infection.

To confirm that DAB and SFN generates ROS and induces oxidative stress within human macrophages, cells were exposed to 10 μM DAB and SFN and 0.5 μM AMB the same concentrations used in the RNA-seq quantification. Intracellular ROS was quantified through DCFDA

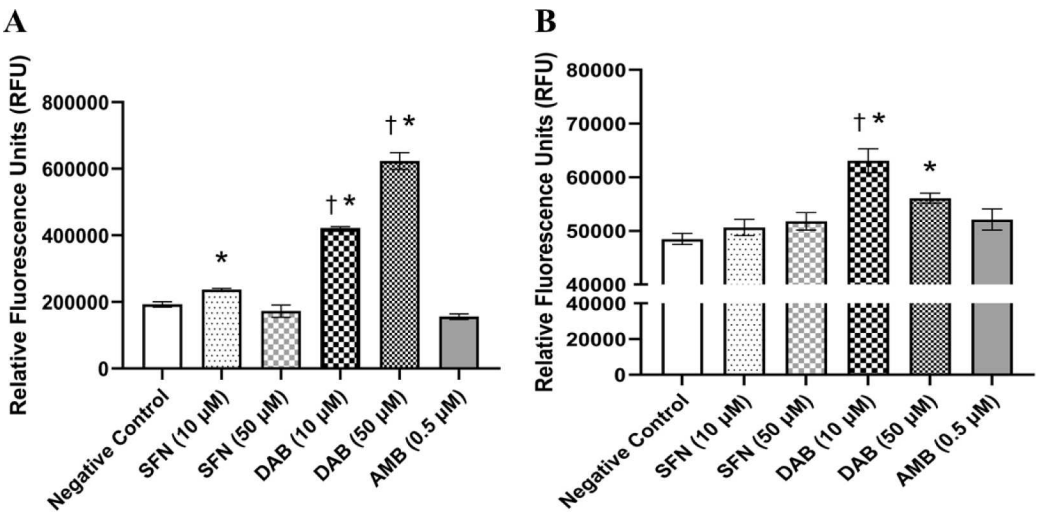

Fig. 5. Increase in reactive oxygen species and mitochondrial superoxide in LD promastigotes exposed to DAB and SFN. Metacyclic promastigotes were incubated with H_2DCFA (A) or MitoSox (B) and then treated with 10 μM or 50 μM of DAB or SFN and 0.5 μM Amphotericin B. Fluorescence was quantified through flow cytometry 24 h post-exposure. Data presented are median fluorescence ± SD (n = 3). Asterisks indicate a significant difference compared to controls cells not exposed to any compound ($P < 0.05$). Daggers indicate a significant difference compared to 10 or 50 μM SFN. The experiment was repeated with three technical replicates (n = 3).

fluorescence via flow cytometry. Both DAB and SFN produced significant intracellular ROS levels after one hour while AMB did not generate ROS (Fig. 6). These data indicate that both SFN and DAB generate host-derived intracellular ROS in THP-1 cells and confirm previous reports that SFN alters redox sensitive cysteine residues on KEAP1 to activate NRF2[30] and that DAB generates ROS [6] and finally that AMB has distinct intracellular effects.[31]

The inhibitory effects of DAB and SFN against the intracellular amastigote form of *Leishmania donovani* was also assessed post-infection as previously described.[15] Adherent, differentiated THP-1 cells were infected with metacyclic promastigotes for 2 h, then incubated with 10 μM of DAB and SFN or 0.5 μM Amphotericin B for an additional 48 h. The lower concentration of DAB and SFN were chosen for the amastigote assay to ensure that changes in oxidative stress occurred in macrophages in the absence of decreased viability. The number of intracellular amastigotes was significantly reduced in the presence of SFN and AMB ($P < 0.05$) (Fig. 7). DAB treatment also led to a reduction in amastigote formation although this reduction was not significant.

Cellular ROS are radical and non-radical oxygen species produced

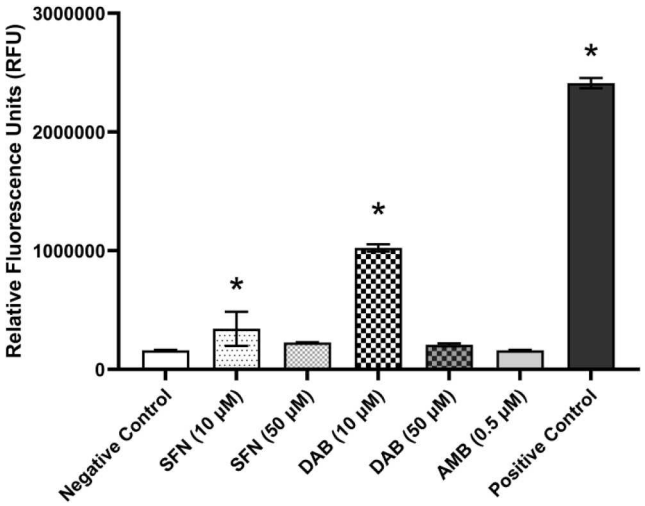

Fig. 6. Increase in oxidative stress in human macrophages exposed to DAB and SFN. Human macrophages were incubated with H_2DCFA and then treated with 10 μM of DAB and SFN or 0.5 μM Amphotericin B. Fluorescence was quantified through flow cytometry 1-hour post-exposure. Data presented are median fluorescence ± SD (n = 3). Asterisks indicate a significant difference compared to controls cells not exposed to any compound ($P < 0.05$). The experiment was repeated at least three times (≥3 biological replicates).

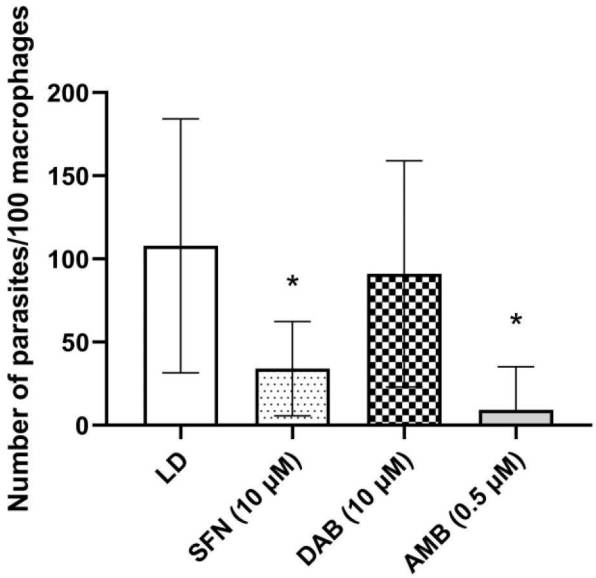

Fig. 7. Intracellular numbers of amastigote *Leishmania donovani* in infected human macrophages. Metacyclic promastigotes infected human differentiated THP-1 cells (10:1 ratio) for 2 h then were exposed to either 10 μM SFN, 10 μM DAB or 0.5 μM AMB for 48 h. Data presented are mean number of amastigotes per 100 THP-1 cells ± SEM. Asterisks indicate a significant difference compared to controls cells not exposed to any compound ($P < 0.05$). The experiment was repeated at least three times (≥3 biological replicates).

from molecular oxygen which include, among others, superoxide anion, hydrogen peroxide and hydroxyl radical.[32] In normal unstressed conditions, they play important roles in cellular signaling by activating the NRF2 pathway.[8] Higher levels of ROS in macrophages during parasitic infections can result in oxidative stress and even cell death.[33] Our data clearly demonstrate that both SFN and DAB treated parasites show an increase in total ROS production. However, the magnitude of the increase significantly differed indicating that DAB was a more potent inducer of ROS and superoxide. Therefore, based on the oxidative stress levels and RNA-seq data, the anti-parasite mechanisms leading to promastigote cell death differ between SFN and DAB. However, both are effective against *Leishmania* infections.

3. Conclusions

This work illustrates the utility of the Meyer-Schuster rearrangement as a key step in the syntheses of bioactive alpinoids. The synthesis of deoxyalpinoid B was completed using a Au (I) catalyzed Meyer-Schuster rearrangement. The synthesis was high yielding, amenable to scale-up, and delivered adequate access to quantities necessary for biological assays. The synthesis of DAB on a gram scale is cost effective given that the synthesis begins with eugenol ($0.09/g from Sigma Aldrich) and that very low catalyst loadings (1 mol%) are required for the Meyer-Schuster rearrangement. Assuming the procedures we report would scale with similar yields, 3.7 g of DAB could be produced using 125 mg of the Au(I) catalysts which costs only $123 from Sigma Aldrich. We are confident that this work could be generalized to the synthesis of other bioactive α,β-unsaturated ketone containing natural products and to the synthesis of alpinoid analogs. These experiments are underway and will be reported in due course.

For the first time, deoxyalpinoid B and an antioxidant inducing compound, sulforaphane, were tested for activity against *Leishmania donovani* and *Leishmania infantatum*, two protozoan, single-celled organisms that cause the neglected tropical disease leishmaniasis. Our current data indicate that both DAB and SFN inhibited promastigote and to a certain extent amastigote viability. Finally, to identify the cell-mediated antileishmanial pathways activated by natural products during LD infection in human macrophages, whole RNA sequence transcription was analyzed in cells infected with LD then exposed to DAB, SFN and amphotericin B. In some cases, these compounds possess antileishmanial activity comparable to amphotericin B, the current standard of care for these infections.

Data presented in this paper are exciting in terms of identifying new antileishmanial compounds and the intracellular pathways activated with compounds, however, this study has limitations. First, it will be necessary to synthesize additional analogs of DAB and show structure–activity-relationships with the potential of identifying more active compounds in the future. For example, future work will focus on the relationship between specific structural features such as alpinoid substitution patterns, presence/absence of the α,β-unsaturated ketone moiety and the isothiocyanate group and their resulting change in antileishmanial activity. Second, the data presented in this paper are focused on human cells grown *in vitro* and are not supported by *in vivo* studies, which would provide data on the immune response post-infection and the associated immune response given different treatments. Previous results obtained with mouse models, specifically parasite species that lead to visceral leishmaniasis (LD and LI), can be influenced by several experimental parameters, such as the mouse genetic background, parasite genotype, inoculation route and parasite dose.[34] Future studies will also identify the most appropriate clinical isolates to test antileishmanial activity in humans. Finally, the premise that oxidative stress and downstream cellular events, such as the activation of the NRF2 transcription factor, lead to decreases in parasite viability is controversial.[26,35,36] Therefore, this hypothesis will need to be further investigated and the specific cellular pathways activated due to oxidative stress (autophagy, protein degradation, etc.) will be identified in future studies.

4. Experimental protocols

General Experimental Procedures. All chemicals (AR grade), except those indicated below, were purchased from Sigma-Aldrich (St. Louis, MO) and used without further purification. RPMI 1640 media, M199 media, fetal bovine serum and antibiotics (penicillin/streptomycin) solution were purchased from Thermo Fisher Scientific (Waltham, MA). CellTiterBlue reagent was purchased from Promega (Madison, WI). Sulforaphane was purchase from LKT laboratories (St. Paul, MN). All solvents were degassed with nitrogen and passed through activated molecular sieves prior to use. Reactions involving air or moisture sensitive reagents or intermediates were performed under an inert atmosphere of nitrogen in glassware that had been oven or flame dried. Reagents were used without further purification unless indicated otherwise. The ^{1}H and ^{13}C NMR spectra were obtained on a Bruker Avance NEO-400 spectrometer, operating at 400 and 100 MHz respectively. Unless indicated otherwise, all spectra were run as solutions in $CDCl_3$. The ^{1}H NMR chemical shifts are reported in parts per million (ppm) downfield from tetramethylsilane (TMS) and are, in all cases, referenced to the residual protio-solvent present (δ 7.24 for $CHCl_3$). The ^{13}C NMR chemical shifts are reported in ppm relative to the center line of the multiplet for deuterium solvent peaks (δ 77.0 (t) for $CDCl_3$).

(4-allyl-2-methoxyphenoxy)triisopropylsilane (4). TIPS-Cl (8.3 g, 43 mmol, 9.1 mL) was added to a solution of eugenol (8.2 g, 50 mmol, 7.7 mL) and imidazole (8.7 g, 131 mmol) in tetrahydrofuran (THF) (40 mL) and the reaction was stirred at room temperature (rt) for 1.5 h. The solvent was removed under vacuum and CH_2Cl_2 (50 mL) was added. The organic layer was washed with 0.5 M HCl (3 × 50 mL), 1 M NaOH (3 × 50 mL), brine (50 mL), dried ($MgSO_4$), and concentrated under reduced pressure to give a yellow oil (12.5 g, 91 %) that was used without further purification; ^{1}H NMR (400 MHz) δ 6.81 (d, J = 8.0 Hz, 1H), 6.68 (d, J = 2.0 Hz, 1H), 6.63 (dd, J = 8.0, 2.0 Hz 1H), 5.98 (comp, 1H), 5.09 (m, 1H), 5.05 (m, 1H), 3.81 (s, 3H), 3.34 (d, J = 6.4 Hz, 2H), 1.26 (sept, J = 7.2 Hz, 3H), 1.11 (d, J = 6.4 Hz, 18H); ^{13}C NMR (100 MHz) δ 150.7, 143.7, 137.9, 133.0, 120.5, 120.2, 115.4, 112.7, 55.5, 39.9, 17.9, 12.9; IR (neat) 2945, 2867, 1513, 1464, 1287, 1234, 914; HRMS (ESI) *m/z* 338.2504 [$C_{19}H_{36}NO_2Si$ (M + NH_4) requires 338.2515].

3-(3-methoxy-4-((triisopropylsilyl)oxy)phenyl)propan-1-ol (5). A solution of I_2 (1.15 g, 4.56 mmol) in THF (10 mL) was added to $NaBH_4$ (350 mg, 9.14 mmol) in THF (15 mL) at 0 °C over 1 h. Then a solution of **4** (5.9 g, 18.3 mmol) in THF (10 mL) was added at 0 °C over 15 min. The ice bath was removed and the reaction was stirred at rt for 2 h·H_2O (2 mL) was added slowly at 0 °C followed by 3 M NaOH (4.6 mL) and 30 % H_2O_2 (1.6 mL). The reaction was stirred at 0 °C for 1 h and then quenched with saturated $Na_2S_2O_3$ (50 mL). The mixture was extracted with EtOAc (3 × 30 mL) and the combined organic layers were washed with brined (50 mL), dried ($MgSO_4$), and concentrated under reduced pressure to give a colorless oil (4.3 g, 70 %) that was used without further purification; ^{1}H NMR (400 MHz) δ 6.80 (d, J = 8.0 Hz, 1H), 6.70 (d, J = 2.4 Hz, 1H), 6.64 (dd, J = 8.0, 2.4 Hz, 1H), 3.81 (s, 3H), 3.68 (t, J = 6.0 Hz, 2H), 2.66 (t, J = 7.6 Hz, 2H), 1.89 (app pent, 2H); 1.26 (sept, J = 7.2 Hz, 3H), 1.10 (d, J = 7.2 Hz, 18H); ^{13}C NMR (100 MHz) δ 150.7, 143.6, 134.9, 120.3, 120.2, 112.5, 62.4, 55.5, 34.4, 31.8, 17.9, 12.9; IR (neat) 3354, 2944, 2867, 1514, 1464, 1286, 910; HRMS (ESI) *m/z* 339.2343 [$C_{19}H_{35}O_3Si$ (M + H) requires 339.2355].

3-(3-methoxy-4-((triisopropylsilyl)oxy)phenyl)propanal (6).[15] Pyridinium chlorochromate (PCC) (1.9 g, 9 mmol) was added to a mixture of **5** (2.0 g, 5.9 mmol) Celite (6 g) and CH_2Cl_2 (30 mL) and the reaction was stirred for 1 h. The mixture was filtered through a short pad of silica and Celite (2 cm) and concentrated under reduced pressure. The residue was purified by flash chromatography eluting with EtOAc/hexane (1:9 to 3:7) to give 1.6 g (79 %) of **7** as a colorless oil; ^{1}H NMR (400 MHz) δ 9.84 (t, J = 1.6 Hz, 1H), 6.80 (d, J = 8.0 Hz, 1H), 6.69 (d, J = 2.0 Hz, 1H), 6.63 (dd, J = 8.0, 2.0 Hz, 1H), 3.81 (s, 3H), 2.91 (t, J = 7.2 Hz, 2H), 2.77 (t, J = 7. 2 Hz, 2H), 1.26 (sept, J = 7.2 Hz, 3H), 1.10 (d, J = 7.2 Hz, 18H).

1-(3-methoxy-4-((triisopropylsilyl)oxy)phenyl)-7-phenylhept-4-yn-3-ol (7). nBuLi (1.78 mL, 2.5 M in hexane) was added to a solution of 4-phenyl-1-butyne (648 mg, 4.97 mmol, 0.7 mL) in THF (10 mL) at 0 °C. The reaction was stirred for 15 min and a solution of **6** (1.1 g, 3.27 mmol) in THF (5 mL) was added dropwise. The reaction stirred at 0 °C for 1 h and was then quenched with sat. NH_4Cl (15 mL). The mixture was extracted with EtOAc (2 × 20 mL) and the combined organic layers were washed with brine (20 mL), dried ($MgSO_4$), and concentrated under reduced pressure. The residue was purified by flash chromatography eluting with EtOAc/hexane (1:9 to 2:8) to give 1.38 g (90 %) of **7** as a colorless oil; ^{1}H NMR (400 MHz) δ 7.34–7.23 (m, 5H), 6.79 (d, J = 8.0

Hz, 1H), 6.68 (d, $J = 2.0$ Hz, 1H), 6.62 (dd, $J = 8.0$, 2.0 Hz, 1H), 4.34 (comp, 1H), 3.81 (s. 3H), 2.87 (t, $J = 7.2$ Hz, 2H), 2.68 (t, $J = 8.0$ Hz, 2H), 2.56 (dt, $J = 8.0$, 2.0 Hz, 2H), 1.96 (m, 2H), 1.68 (d, $J = 5.2$ Hz, 1H), 1.26 (sept, $J = 7.2$ Hz, 3H), 1.11 (d, $J = 7.2$ Hz, 18H) ^{13}C NMR (100 MHz) δ 150.7, 143.7, 140.6, 134.5, 128.5, 128.4, 126.3, 120.4, 120.2, 112.6, 85.1, 81.9. 62.1, 55.5, 39.7, 35.0, 31.0, 20.9, 17.9, 12.9; IR (neat) 3380, 2944, 2866, 1514, 1286, 909; HRMS (ESI) *m/z* 484.3230 [$C_{29}H_{46}NO_3Si$ (M + NH_4) requires 484.3247].

(*E*)-7-(3-methoxy-4-((triisopropylsilyl)oxy)phenyl)-1-phenyl-hept-4-en-3-one (8). PPh_3AuNTf_2 (8 mg, 0.0053 mmol) was added to a solution of **7** (247 mg, 0.53 mmol) and MeOH (0.02 mL, 0.53 mmol) in toluene (0.5 mL). The reaction stirred at rt for 1.5hr and was concentrated under reduced pressure. The residue was purified by flash chromatography eluting with EtOAc/hexane (1:19 to 1:9) to give 221 mg (89 %) of **8** as a colorless oil; ^{1}H NMR (400 MHz) δ 7.33–7.20 (m, 5H), 6.88–6.80 (m, 2H), 6.65 (d, $J = 2.0$ Hz, 1H), 6.61 (dd, $J = 8.0$, 2.0 Hz, 1H), 6.11 (d, $J = 16.0$ Hz, 1H), 3.80 (s, 3H), 2.95 (m, 2H), 2.85 (m, 2H), 2.72 (t, $J = 7.2$ Hz, 2H), 2.51 (m, 2H), 1.26 (sept, $J = 7.2$ Hz, 3H), 1.10 (d, $J = 7.2$ Hz, 18H); ^{13}C NMR (100 MHz) δ 199.4, 150.7, 146.5, 143.9, 141.3, 133.8, 130.7, 128.5, 128.4, 126.1, 120.3, 120.3, 112.4, 55.5, 41.7, 34.4, 34.1, 30.0, 17.9, 12.9; IR (neat) 2944, 2867, 1674, 1514, 1286, 909; HRMS (ESI) *m/z* 489.2800 [$C_{29}H_{42}NaO_3Si$ (M + Na) requires 489.2801].

Deoxyalpinoid B (1). A solution of TBAF (0.321 mL, 1 M in THF, 0.321 mmol) was added to a solution of **8** (100 mg, 0.214 mmol) in THF (1 mL) at 0 °C. The reaction was stirred at 0 °C and quenched with sat. NH_4Cl (5 mL). The mixture was extracted with EtOAc (3 × 15 mL) and the combined organic layers were washed with brine (20 mL), dried ($MgSO_4$), and concentrated under reduced pressure. The residue was purified by flash chromatography eluting with EtOAc/hexane (2:8) to give 54 mg (82 %) of **1** as a colorless oil; ^{1}H NMR (400 MHz) δ 7.33–7.21 (m, 5H), 6.89–6.83 (m, 2H), 6.70–6.69 (m, 2H), 6.14 (d, $J = 16.0$ Hz, 1H), 5.62 (s, 1H), 3.89 (s, 3H), 2.96 (m, 2H), 2.88 (m, 2H), 2.72 (t, $J = 8.0$ Hz, 2H), 2.52 (m, 2H); ^{13}C NMR (100 MHz) δ 199.4, 146.4, 144.0, 141.1, 132.5, 130.6, 128.4, 128.3, 126.0, 120.8, 114.3, 110.8, 55.8, 41.7, 34.4, 34.0, 30.0; IR (neat) HRMS (ESI) *m/z* 311.1641 [$C_{20}H_{23}O_3$ (M + H) requires 311.1647].

***Leishmania* and Human Macrophage Cell Culture.** *Leishmania donovani* (LD) strain MHOM/IN/DD8*, L. infantatum* strain MHOM/TN/80/IPT-1 (LI) and the THP-1 human monocytic cell line were purchased from ATCC (Manassas, VA). LD and LI were cultured in 10 % FBS with antibiotics in M199 media. LD and LI cultures were maintained in 50 mL conical at 25C, checked weekly for purity and subculture once every-five days when the number of metacyclic promastigotes were at the highest concentrations. THP-1 cells were maintained in 10 % FBS with antibiotics in RPMI at 37C in 5 % CO_2. Cells were passaged and subcultured when cell concentrations reached>8x10^5 cells/mL, which occurred usually every-three days.

THP-1 Viability Assay. THP-1 cells (50,000 cells per well) were cultured in the presence of various concentrations of SFN and DAB (1–100 μM SFN or DAB) for 48 h (n = 5–10 technical replicates). RPMI media was used as a negative control. CellTiterBlue was added and incubated 3 h at 37 °C. Fluorescence was measured at ($560_{Ex}/590_{Em}$) in an Infinite 200 PRO series plate reader (Tecan Systems Inc., San Jose, CA). Percent viability was calculated using the following equation: percent viability = (100 – (Mean fluorescence of control – fluorescence of sample)/ Mean fluorescence of control cells*100. The experiment was repeated at least four times (≥4 biological replicates). Each data point represented a mean (±SD) and was normalized to the value of the corresponding control cells.

Promastigote Viability Assay. LD and LI promastigotes in the infective metacyclic stage (long cylindrical forms, ~ 5–6 day old cultures), approximately 1 million LD/LI cells per well, were cultured in the presence of either 0.5 μM amphotericin B, 10–50 μM SFN or 10–50 μM deoxyalpinoid B for 48 h (n = 5–10 technical replicates). CellTiterBlue was added and incubated 3 h at 37 °C. Fluorescence was measured at ($560_{Ex}/590_{Em}$) in an Infinite 200 PRO series plate reader (Tecan Systems Inc., San Jose, CA). The experiment was repeated at least four times (≥4 biological replicates). Each data point represented a mean (±SD) and was normalized to the value of the corresponding control cells. Amphotericin B was used as the positive control[19] and M199 media was used as the negative control.

Assessment of Intracellular Antileishmanial Activity: THP-1 cells were differentiated into macrophage-like cells for 18 h with phorbol 12-myristate 13-acetate (PMA) as previously described.[19] Phorbol 12-myristate 13-acetate (PMA) was added to diluted cell culture suspension (10 μl/20 mL culture from the stock of 50 μg/ml in DMSO) to reach a final PMA concentration in diluted cells culture of 25 ng/ml. Briefly, 5-day old metacyclic promastigotes were used to infect adherent macrophages at a 10:1 ratio (promastigotes to human macrophages) for 2 h in RPMI media at 37 °C. Cells were washed twice with PBS to remove unattached promastigotes and then incubated with either 0.5 μM amphotericin B, 10 μM SFN or 10 μM deoxyalpinoid B for 48 h (n = 3 technical replicates). Cells were washed with PBS twice, fixed with 4 % paraformaldehyde, and permeabilized. Nuclei were identified by staining with DAPI. All samples were blinded prior to image acquisition. All images were obtained with an Olympus IX50 inverted microscope. Human macrophages (large nuclei) and amastigote (small punctate nuclei) were enumerated as blinded samples to quantify the number of amastigotes per 100 THP-1 cells. Amphotericin B was used as the positive control[19] and M199 media was used as the negative control. The experiment was repeated at least three times (≥3 biological replicates).

Macrophage Derived Reactive Oxygen Species (ROS) Quantification: THP-1 cells were incubated with 10 μM 2′,7′-dichlorodihydrofluorescein diacetate (H_2DCFDA) (Molecular Probes) for 30 min at 37 °C. Cells were washed with PBS and exposed to SFN, DAB and AMB at various concentrations for 60 min. Hydrogen peroxide (0.03 %) was used as a positive control. Green fluorescence was quantified on a BD C6 Accuri flow cytometer using a 488 nm excitation wavelength and an emission filter of 533 nm ± 30 nm (BD Biosciences). 50,000 events were collected (n = 3 technical replicates per condition). The experiment was repeated at least three times (≥3 biological replicates).

Promastigote Reactive Oxygen Species (ROS) Quantification: Total ROS production within LD promastigotes was determined after 24 h of treatment with SFN (10 and 50 μM), DAB (10 and 50 μM) and AMB (0.5 μM) as previously described.[37] Briefly, metacyclic promastigotes were washed, resuspended in PBS and 5 × 10^6 parasites/ml were incubated with H_2DCFDA probe (D399) (10 μM) (Invitrogen, Molecular Probes, Eugene, Oregon) for 30 min in the dark at room temperature. Green fluorescence was quantified on a BD C6 Accuri flow cytometer using a 488 nm excitation wavelength and an emission filter of 533 nm ± 30 nm (BD Biosciences). 20,000 events were collected (n = 3 technical replicates per condition).

Mitochondrial Superoxide Quantification: Mitochondrion-generated ROS within LD promastigotes was determined after 24 h of treatment with SFN (10 and 50 μM), DAB (10 and 50 μM) and AMB (0.5 μM) as previously described.[34] Briefly, metacyclic promastigotes were washed, resuspended in PBS and 5 × 10^6 parasites/ml were incubated with MitoSOX Red reagent (5 μM) (Invitrogen, Molecular Probes, Eugene, Oregon) for 30 min in the dark at room temperature. Red fluorescence was quantified on a BD C6 Accuri flow cytometer using a 488 nm excitation wavelength and an emission filter of 585 nm ± 40 nm (BD Biosciences). 20,000 events were collected (n = 3 technical replicates per condition).

RNA isolation, Illumina RNA-sequencing and quantification of differential gene expression and pathway analysis. THP-1 cells were treated with PMA (25 ng/ml final concentration) and cultured overnight to allow differentiation and adherence. Cells were challenged with infective metacyclic stage LD (long cylindrical forms, ~ 5 day old culture) at a ratio of 10 LD cells to 1 THP-1 cell or vehicle control in 2 % FBS in RPMI for 4.5 h. Cells were washed with PBS then incubated with either 0.5 μM amphotericin B, 10 μM SFN or 10 μM deoxyalpinoid B for

18 h (n = 4 technical replicates). Cells were washed with PBS and total RNA was isolated using the RNeasy Mini Kit according to the manufacturer's recommended protocol (Qiagen Inc., Valencia, CA). Total RNA purity from the seven experimental groups (No treatment +/− LD, SFN +/− LD, DAB +/− LD, AMB + LD) was checked using the NanoPhotometer NP80 spectrophotometer (IMPLEN, CA, USA). Sequencing libraries (poly A enrichment) were generated by Novogene (Davis, CA). Briefly, messenger RNA was purified from total RNA using poly-T oligo-attached magnetic beads. After fragmentation, the first strand cDNA was synthesized using random hexamer primers followed by the second strand cDNA synthesis. The library was ready after end repair, A-tailing, adapter ligation, size selection, amplification, and purification. The library was checked with Qubit and real-time PCR for quantification and bioanalyzer for size distribution detection. Quantified libraries were pooled and sequenced according to effective library concentration and data amount through the Illumina platform using the NovaSeq PE150 strategy. The expected number of Fragments Per Kilobase of transcript sequence per Millions base pairs sequenced (FPKM) was used to estimate gene expression levels.

Both the principal components analysis (PCA) plots and the Pearson's correlation heat map were generated using normalized reads per kilobases of transcript per 1 million mapped reads (RPKM) count as previously described (Koch 2018). The square of the Pearson correlation coefficient of all biological replicates were >0.9. The variation within each experimental group in the entire dataset was also analyzed via principal components (PCs). The PCA demonstrated expected grouping among replicates within samples and sample groups spread across the two PCs. PC1 accounted for 16.19 % of the variance, and PC2 accounted for an additional 46.55 % of the variance.

Genes with an adjusted *P*-value (padj) < 0.05 normalized by DESeq were initially assigned as differentially expressed. The padj value is the transformation of the p value after accounting for multiple testing. The padj takes in to account the false discovery rate (FDR) of p-value, also called a qvalue. An FDR-adjusted p-value of 0.05 implies that we are willing to accept that 5 % of the tests found to be statistically significant (e.g. by p-value) will be false positives. The baseline is 0.05 (a padj < 0.05 is significant). All differentially expressed genes, Kyoto Encyclopedia of Genes and Genomes (KEGG) enrichment pathways and Gene Ontology (GO) enrichment analysis reported herein had an adjusted *P*-value < 0.005, a *P*-value < 0.0005 and a log2 FC > 2 (upregulated) or a log2 FC < -2 (downregulated).

Statistical analysis: Data are given as mean ± SEM. Analyses were done using the software package GraphPad Prism 3.03 (GraphPad, San Diego, CA). One-way ANOVA was used to compare groups with one independent variable. A Dunnett's posttest was used to compare different treatments. To determine if the data are normally distributed a normality test was performed with a post-hoc Shapiro-Wilk test. The number of intracellular amastigotes in all groups was not normally distributed after performing a Shapiro-Wilk test. Significance was noted at $P < 0.05$.

CRediT authorship contribution statement

Emma Leary: Formal analysis, Investigation, Visualization, Writing – review & editing. **Ethan T. Anderson:** Investigation, Visualization, Writing – review & editing. **Jasmine K. Keyes:** Investigation, Writing – review & editing. **Tristan R. Huskie:** Investigation, Writing – review & editing. **David J. Blake:** Conceptualization, Formal analysis, Methodology, Project administration, Supervision, Visualization, Writing – original draft, Writing – review & editing. **Kenneth A. Miller:** Conceptualization, Formal analysis, Methodology, Project administration, Supervision, Visualization, Writing – original draft, Writing – review & editing.

Declaration of Competing Interest

The authors declare that they have no known competing financial interests or personal relationships that could have appeared to influence the work reported in this paper.

Data availability

No data was used for the research described in the article.

Acknowledgements

The authors would like to thank the NIH SCORE grant, NIH-BLaST program at the University of Alaska-Fairbanks, and Fort Lewis College for financial support. This research was supported by an NIH-URISE award (T34GM140909) for J.K. BLaST is supported by the NIH Common Fund, through the Office of Strategic Coordination, Office of the NIH Director with the linked awards: TL4GM118992, RL5GM118990, & UL1GM118991 and supported E.L and E.A. Research reported in this publication was also supported by the National Institute of General Medical Sciences of the National Institutes of Health under Award Number SC3GM141838. The content is solely the responsibility of the authors and does not necessarily represent the official views of the National Institutes of Health. This research was supported by a National Science Foundation – Major Research Instrumentation award (2017945). The authors wish to thank the Analytical Resources Core (RRID: SCR_021758) at Colorado State University for instrument access, training and assistance with sample analysis.

Appendix A. Supplementary material

Supplementary data to this article can be found online at https://doi.org/10.1016/j.bmc.2022.117136.

References

[1] Alvar J, Vélez ID, Bern C, et al. The WHO Leishmaniasis Control Team. Leishmaniasis worldwide and global estimates of its incidence. *PLoS One*. 2012;7:e35671.
[2] Lindoso JAL, Costa JML, Queiroz IT, Goto, H. Review of the current treatments for leishmaniases. 2012,3: 69–77. https://doi.org/10.2147/RRTM.S24764.
[3] Jhingran A, Chawla B, Saxena S, Barrett MP, Madhubala R. Paromomycin: uptake and resistance in *Leishmania* donovani. *Mol Biochem Parasitol*. 2009;164:111–117. https://doi.org/10.1016/j.molbiopara.2008.12.007.
[4] Dayakar A, Chandrasekaran S, Veronica J, Sundar S, Maurya R. *In vitro* and *in vivo* evaluation of anti-leishmanial and immunomodulatory activity of Neem leaf extract in *Leishmania donovani* infection. *Expe Parasitol*. 2015;153:45–54. https://doi.org/10.1016/j.exppara.2015.02.011.
[5] Sun Y, Tabata K, Matsubara H, Kitanaka S, Suzuki T, Yasukawa K. New Cytotoxic Diarylheptanoids from the Rhizomes of *Alpinia officinarum*. *Planta Med*. 2008;74:427–431. https://doi.org/10.1055/s-2008-1034345.
[6] Gamre S, Tyagi M, Chatterjee S, Patro BS, Chattopadhyay S, Goswami D. Synthesis of bioactive Diarylheptanoids from *Alpinia officinarum* and their mechanism of action for anticancer properties in breast cancer cells. *J Natural Prod*. 2021;84:352–363. https://doi.org/10.1021/acs.jnatprod.0c01012.
[7] Fahey JW, Talalay P. Antioxidant functions of sulforaphane: a potent inducer of Phase II detoxication enzymes. *Food Chem Toxicol*. 1999;37:973–979. https://doi.org/10.1016/s0278-6915(99)00082-4.
[8] Kensler TW, Wakabayashi N, Biswal S. Cell survival responses to environmental stresses via the Keap1-Nrf2-ARE pathway. *Annu Rev Pharmacol Toxicol*. 2007;47:89–116. https://doi.org/10.1146/annurev.pharmtox.46.120604.141046.
[9] Dinkova-Kostova AT, Holzclaw WD, Cole RN, et al. Direct evidence that sulfhydryl groups of Keap1 are the sensors regulating induction of phase 2 enzymes that protect against carcinogens and oxidants. *Proc Natl Acad Sci*. 2002;99:11908–11913. https://doi.org/10.1073/pnas.172398899.
[10] Hu C, Eggler AL, Mesecar AD, van Breemen RB. Modification of Keap1 cysteine residues by sulforaphane. *Chem Res Toxicol*. 2011;24:515–521. https://doi.org/10.1021/tx100389r.
[11] Thimmulappa RK, Mai KH, Srisuma S, Kensler TW, Yamamoto M, Biswal S. Identification of Nrf2-regulated genes induced by the chemopreventive agent sulforaphane by oligonucleotide microarray. *Cancer Res*. 2002;62:5196–5203.
[12] Starrett W, Blake DJ. Sulforaphane inhibits de novo synthesis of IL-8 and MCP-1 in human epithelial cells generated by cigarette smoke extract. *J Immunotoxicol*. 2011;8:150–158. https://doi.org/10.3109/1547691X.2011.558529. PMID: 21401388.

[13] Salih Q, Beaudry CM. Chirality in dirarylether heptanoids: synthesis of myricatomentogenin, jugacathanin, and congeners. *Org Lett*. 2012;14:4026–4029. https://doi.org/10.1021/ol301893t.
[14] Engel DA, Dudley GB. The Meyer-Schuster rearrangement for the synthesis of α,β-unsaturated carbonyl compounds. *Org Biomol Chem*. 2009;7:4149–4158. https://doi.org/10.1039/b912099h.
[15] Keyes JK, Butzke MB, Miller KA. Efficient total synthesis of three alpinoids via the Au(I)-catalyzed Meyer-Schuster rearrangement. *Tetrahedron Lett*. 2022;104: 154105. https://doi.org/10.1016/j.tetlet.2022.154015.
[16] Li Z, Tong R. Catalytic environmentally friendly protocol for Achmatowicz rearrangement. *J Org Chem*. 2016;81:4847–4855. https://doi.org/10.1021/acs.joc.6b00469.
[17] Pennel MN, Unthank MG, Turner P, Sheppard TD. A general procedure for the synthesis of enones via gold-catalyzed meyer-schuster rearrangement of propargylic alcohols at room temperature. *J Org Chem*. 2011;76:1479–1482. https://doi.org/10.1021/jo102263t.
[18] Itokawa H, Morita M, Mihashi S. two new Diarylheptanoids from *Alpinia officinarum* Hance. *Chem Pharm Bull*. 1981;29:2383–2385. https://doi.org/10.1248/cpb.29.2383.
[19] Jain SK, Sahu R, Walker LA, Tekwani BL. A parasite rescue and transformation assay for antileishmanial screening against intracellular Leishmania donovani amastigotes in THP1 human acute monocytic leukemia cell line. *J Vis Exp*. 2012; 70:e4054.
[20] Vermeersch M, Inocêncio de Luz R, Toté K, Timmermans JP, Cos P, Maes L. In vitro susceptibilities of Leishmania donovani promastigote and amastigote stages to antileishmanial reference drugs: practical relevance of stage-specific differences. *Antimicrob Agents Chemotherapeut*. 2009;53:3855–3859. https://doi.org/10.1128/AAC.00548-09.
[21] Mbongo N, Loiseau PM, Billion MA, Robert-Gero M. Mechanism of amphotericin B resistance in Leishmania donovani promastigotes. *Antimicrob Agents Chemotherapeut*. 1998;42:352–357. https://doi.org/10.1128/AAC.42.2.352.
[22] Sahoo GC, Rani M, Dikhit MR, Ansari WA, Das P. Structural Modeling, Evolution and Ligand Interactions of KMP11 Protein of Different *Leishmania* Strains. *J Comput Sci Syst Biol*. 2009;2:147–158. https://doi.org/10.4172/jcsb.1000026.
[23] Gómez MA, Navas A, Márquez R, et al. Leishmaniapanamensis infection and antimonial drugs modulate expression of macrophage drug transporters and metabolizing enzymes: impact on intracellular parasite survival. *J Antimicrob Chemother*. 2014;69:139–149. https://doi.org/10.1093/jac/dkt334.
[24] Barrera MC, Rojas LJ, Weiss A, et al. Profiling gene expression of antimony response genes in *Leishmania (Viannia) panamensis* and infected macrophages and its relationship with drug susceptibility. *Acta Trop*. 2017;176:355–363. https://doi.org/10.1016/j.actatropica.2017.08.017.
[25] Ruttkay-Nedecky B, Nejdl L, Gumulec J, et al. The Role of Metallothionein in Oxidative Stress. *Int J Mol Sci*. 2013;14:6044–6066. https://doi.org/10.3390/ijms14036044.
[26] Saha S, Roy S, Dutta A, Jana K, Ukil A. *Leishmania donovani* Targets Host Transcription Factor NRF2 To Activate Antioxidant Enzyme HO-1 and Transcriptional Repressor ATF3 for Establishing Infection. *Infect Immun*. 2021;89: e00764–e820. https://doi.org/10.1128/IAI.00764-20.
[27] Nishinaka T, Miura T, Okumura M, Nakao F, Nakamura H, Terada T. Regulation of aldo-keto reductase AKR1B10 gene expression: involvement of transcription factor Nrf2. *Chem Biol Interact*. 2011;191:185–191. https://doi.org/10.1016/j.cbi.2011.01.026.
[28] Wan S, Pan Q, Yang G, Kuang J, Luo S. Role of CYP4F2 as a novel biomarker regulating malignant phenotypes of liver cancer cells via the Nrf2 signaling axis. *Oncol Lett*. 2020;20:e11874.
[29] Singh A, Misra V, Thimmulappa RK, et al. Dysfunctional KEAP1-NRF2 interaction in non-small-cell lung cancer. *PLoS Med*. 2006;3:e420.
[30] Choi WY, Choi BT, Lee WH, Choi YH. Sulforaphane generates reactive oxygen species leading to mitochondrial perturbation for apoptosis in human leukemia U937 cells. *Biomed Pharmacother*. 2008;62:637–644. https://doi.org/10.1016/j.biopha.2008.01.001.
[31] Brajtburg J, Powderly WG, Kobayashi GS, Medoff G. Amphotericin B: current understanding of mechanisms of action. *Antimicrob Agents Chemother*. 1990;34: 183–188. https://doi.org/10.1128/aac.34.2.183.
[32] Liou GY, Storz P. Reactive oxygen species in cancer. *Free Radic Res*. 2010;44: 479–496. https://doi.org/10.3109/10715761003667554.
[33] Maldonado E, Rojas DA, Urbina F, Solari A. The oxidative stress and chronic inflammatory process in Chagas disease: role of exosomes and contributing genetic factors. *Oxid Med Cell Longev*. 2021;4993452. https://doi.org/10.1155/2021/4993452.
[34] Marques F, Vale-Costa S, Cruz T, et al. Studies in the mouse model identify strain variability as a major determinant of disease outcome in Leishmania infantum infection. *Parasit Vectors*. 2015;8:644. https://doi.org/10.1186/s13071-015-1259-6.
[35] Vivarni Á, Calegari-Silva TC, Saliba AM, et al. Systems approach reveals nuclear factor erythroid 2-related factor 2/protein kinase R crosstalk in human cutaneous Leishmaniasis. *Front Immunol*. 2017;8:1127. https://doi.org/10.3389/fimmu.2017.01127.
[36] de Menezes JPB, Khouri R, Oliveira CVS, et al. Proteomic analysis reveals a predominant NFE2L2 (NRF2) signature in canonical pathway and upstream regulator analysis of *Leishmania*-infected macrophages. *Front Immunol*. 2019;10: 1362. https://doi.org/10.3389/fimmu.2019.01362.
[37] Meinela RS, Almeidab AC, Stroppaa PHF, Glanzmanna N, Coimbrab ES, da Silvaa AD. Novel functionalized 1,2,3-triazole derivatives exhibit antileishmanial activity, increase in total and mitochondrial-ROS and depolarization of mitochondrial membrane potential of Leishmania amazonensis. *Chem Biol Interact*. 2020;315:108850. https://doi.org/10.1016/j.cbi.2019.108850.